1997

Paleoseismicity Of the North Branch Of the Newport-Inglewood Fault Zone In Huntington Beach, California, From Cone Penetrometer Test Data

Lisa B. Grant
Chapman University

John T. Waggoner
Southern California Earthquake Center

Thomas K. Rockwell
Southern California Earthquake Center

Carmen von Stein
Southern California Earthquake Center

Paleoseismicity Of the North Branch Of the Newport-Inglewood Fault Zone In Huntington Beach, California, From Cone Penetrometer Test Data

THE SEISMOLOGICAL SOCIETY OF AMERICA
400 Evelyn Ave., Suite 201
Albany, CA 94706-1375
(510) 525-5474; FAX (510) 525-7204
www.seismosoc.org

Bulletin of the Seismological Society of America, Vol. 87, No. 2, pp. 277–293, April 1997

Paleoseismicity of the North Branch of the Newport–Inglewood Fault Zone in Huntington Beach, California, from Cone Penetrometer Test Data

by Lisa B. Grant,* John T. Waggoner, Thomas K. Rockwell, and Carmen von Stein

Abstract Application of cone penetrometer testing (CPT) is a promising method for studying subsurface fault zones in stratified, unconsolidated sediment where trenching is not feasible. Analysis of data from 72 CPTs, spaced 7.5 to 30.0 m apart, and 9 borings indicates that the North Branch fault, the active strand of the Newport–Inglewood fault zone (NIFZ) in Huntington Beach, has generated at least three and most likely five recognizable surface ruptures in the past 11.7 ± 0.7 ka. Additional smaller earthquakes similar to the M_w 6.4 1933 Long Beach earthquake may also have occurred but would not be recognizable with this method. The minimum right-lateral Holocene slip rate of the NIFZ in the study area is estimated to be 0.34 to 0.55 mm/yr. The actual slip rate may be significantly higher.

Introduction

The destructive seismic potential of the Newport–Inglewood fault zone (NIFZ) was demonstrated by the damaging 1933 M_w 6.4 Long Beach earthquake, located 8 to 12 km beneath southern Huntington Beach (Hauksson and Gross, 1991). A future major earthquake along the densely populated NIFZ poses one of the greatest hazards to lives and property in the nation (California Division of Mines and Geology, 1988).

Despite historic seismic activity along the NIFZ, the seismic source characteristics of the NIFZ are poorly constrained. Paleoseismic data on the Holocene behavior of the NIFZ and its prehistoric earthquakes are difficult to obtain because most of the Holocene deposits along the fault zone either are obscured by urban development or are located near sea level where a high water table precludes traditional paleoseismic trench investigation. To overcome these obstacles, we used the cone penetrometer test (CPT) method to investigate the Holocene earthquake history of the primary active trace, the North Branch fault (NBF), of the NIFZ in Huntington Beach, California.

Geologic and Tectonic Setting

The NIFZ is the northern part of a zone of coastal strike-slip faults and associated folds extending between Los Angeles and San Diego (Fig. 1). The NIFZ is a major tectonic boundary in southern California (Hill, 1971; Wright, 1991). The northern NIFZ extends along the western margin of the Los Angeles basin from Beverly Hills to Newport Beach. The fault zone continues offshore to the south and then comes ashore again near San Diego as the Rose Canyon fault.

At the surface, the NIFZ is marked by a series of domal uplifts and low mesas arranged in an *en echelon* pattern within a right-lateral strike-slip fault zone (Wilcox *et al.*, 1973; Barrows, 1974; Wright, 1991). The fault zone consists of a complex series of discontinuous strike-slip traces and shorter subsidiary normal and reverse faults (Barrows, 1974; Bryant, 1988). Right-lateral displacement of late-Miocene through late-Pliocene sediments and structural features indicate that strike-slip faulting initiated during the late Pliocene in the Inglewood oil field and earlier along the southern portion of the NIFZ (Freeman *et al.*, 1992). In the Huntington Beach area, right-lateral offset of late-Miocene rocks across the zone may total more than 9.5 km (Hazenbush and Allen, 1958; Bryant, 1988). Displacement of late-Miocene and younger sediments indicates that the long-term right-lateral slip rate of the NIFZ is approximately 0.5 mm/yr (Freeman *et al.*, 1992).

Evidence of tectonic and seismic activity is present along the NIFZ in the form of Quaternary folds, recent faults, and recorded seismicity (Barrows, 1974; Bryant, 1988; Wright, 1991). The Holocene and Quaternary slip rates of the NIFZ are poorly constrained; estimates of the Quaternary slip rate of the NIFZ range from 0.03 to 6.0 mm/yr (Suppe *et al.*, 1992; Petersen and Wesnousky, 1994). In San Diego, the strike-slip Rose Canyon fault has a Holocene slip rate of 1.1 to 2.0 mm/yr (Lindvall and Rockwell, 1995). In the Los Angeles basin, the minimum horizontal Quaternary slip rate across the NIFZ has been estimated at 0.03 to 0.05 mm/yr at Signal Hill in Long Beach (Suppe *et al.*, 1992). However, the 1933 earthquake, which ruptured a 13- to 16-km-long

*Corresponding author.
All authors are participants in the Earthquake Geology Group of the Southern California Earthquake Center.

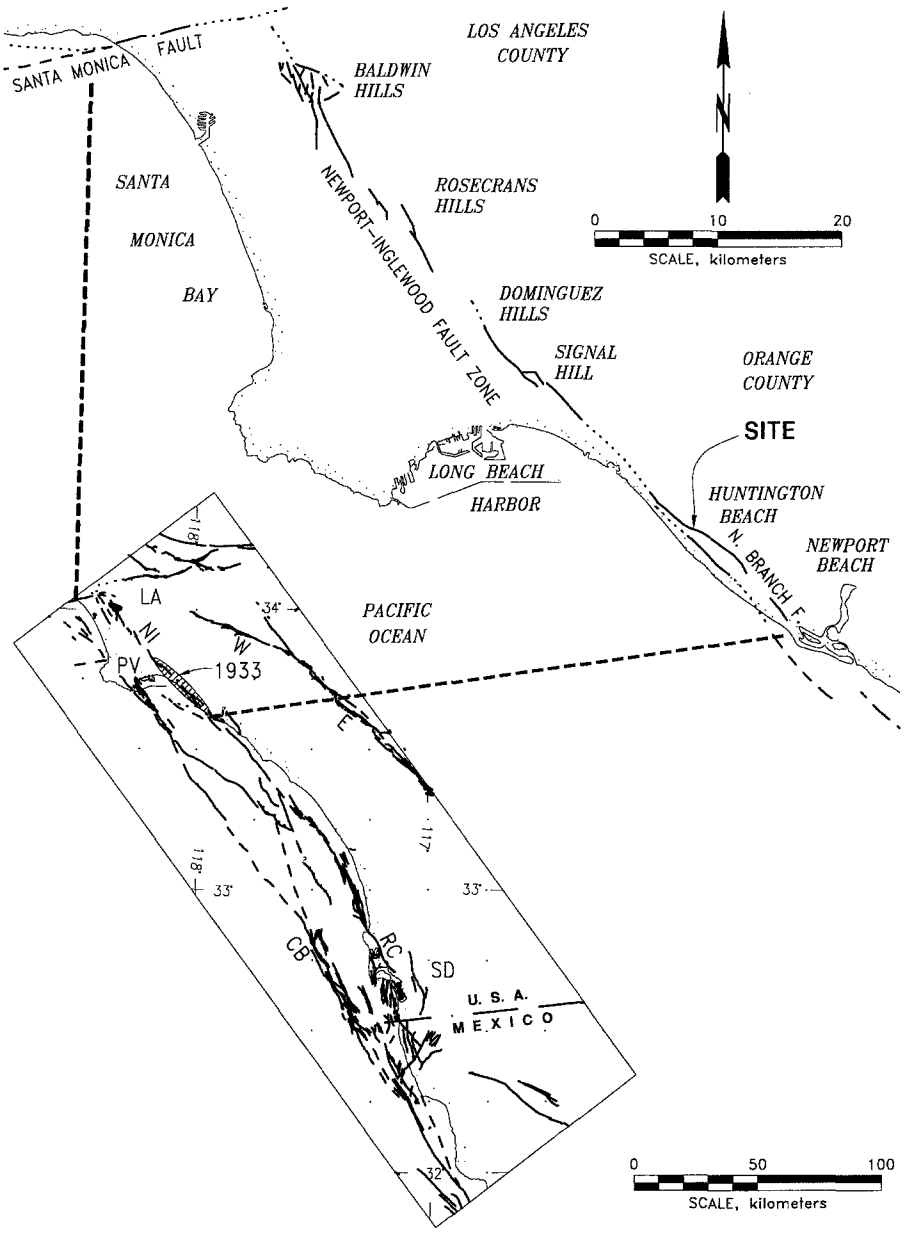

Figure 1. (Inset) Regional tectonic map of coastal southern California showing Newport–Inglewood fault zone (NI), 1933 rupture zone (hatched), Rose Canyon fault (RC), Palos Verdes fault (PV), offshore Coronado Bank fault (CB), Whittier fault (W), Elsinore fault (E), Los Angeles (LA), and San Diego (SD). Modified from Lindvall and Rockwell (1995). (Top) Regional map of the Newport–Inglewood fault zone showing selected faults and Quaternary uplifts marked by hills. Modified from Guptill and Heath (1981).

section of the NIFZ between Long Beach and Newport Beach (Hauksson and Gross, 1991), demonstrated that the southern half of the NIFZ is active and capable of generating significant earthquakes (Hauksson, 1987). The recorded seismicity of the NIFZ and the Holocene slip rate of the Rose Canyon fault suggests that the Holocene slip rate of the NIFZ may be substantially higher than 0.03 to 0.05 mm/yr.

Study Site

We conducted paleoseismic investigations at a site along the North Branch fault (NBF) of the NIFZ. The NBF is the active trace of the NIFZ in Huntington Beach as defined by Bryant (1988). We selected this site because it is close to the epicenter of the 1933 earthquake and because it is one of the few accessible, relatively undisturbed sites along the NIFZ with enough Holocene sediments and correlatable stra-

tigraphy suitable for paleoseismic investigation. In addition, the structure and sedimentation rate at the site have created a good geologic environment for preserving a Holocene record of paleoseismicity.

Within the Huntington Beach oil field, a section of the NBF steps to the right within the study area, as shown in Figure 2. The site topography is nearly flat, and the water table is approximately coincident with the ground surface. Analysis of oil-well E-logs, water-well logs, and CPT data shows that the step-over forms a structural depression, or graben, between the main traces of the fault zone, as shown in Figure 2 (Freeman *et al.,* 1992; California Dept. of Water Resources, 1968). The sense of separation of Miocene through Holocene sediments indicates that faults within the graben have significant normal and strike-slip components of motion. A normal component of motion along the graben boundary faults has created paleoscarps within the Holocene sedimentary section.

During the Holocene, subsidence within the graben caused a locally higher rate of sedimentation. Stratified, unconsolidated sand, silt, clay, and gravel deposits of Holocene age overlie more consolidated Pleistocene age sediments at the site (Woodward-Clyde Consultants, 1987, 1991; Freeman *et al.* 1992; California Dept. of Water Resources, 1968). The Holocene sediments are interpreted to be fluvial, littoral, and estuarine deposits correlative with regional coastal Holocene deposits in Orange and Los Angeles counties (Poland *et al.,* 1956). These sediments are related to rapid global sea-level rise in the early to middle Holocene (Bard *et al.,* 1990; Chappell and Polach, 1991; Gibb, 1986).

Investigation Methods

Several subsurface exploration methods were used to investigate the sediments and analyze the geologic record of faulting at the study site. First, the Holocene traces of the NBF were located by preliminary studies (Woodward-Clyde Consultants, 1987; Freeman *et al.,* 1992). Faults were identified by interpreting oil-well E-logs to define the deep geologic structure, by conducting marine and terrestrial seismic reflection profiles to identify shallower structures, by studying air photos and water-well logs, and by analyzing data from CPTs and borings. Preliminary analysis of stratigraphy and structure was used to select a promising site for detailed study. An area spanning the northeastern boundary of the graben was selected for detailed analysis because it contains laterally correlatable stratigraphy and exhibits a significant apparent vertical component of motion across the graben-

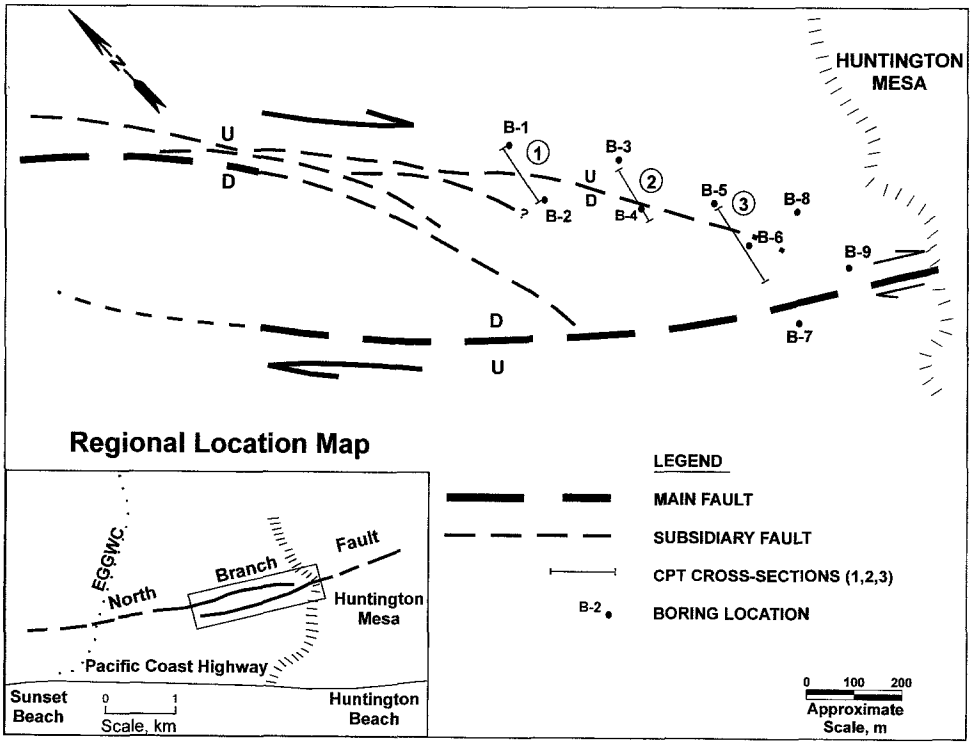

Figure 2. Map of main and subsidiary fault traces; cross sections 1, 2, and 3; and borings at the study site. The site elevation is <1 m. (Elevations of CPT holes and borings are on cross sections.) A right step-over in the right-lateral fault zone creates a structural depression formed by faults with a normal component of motion. Sense of movement of faults is shown by arrows and letters U (up) and D (down). Inset map shows location of study site relative to cultural and geomorphic features. EGGWC is the East Garden Grove Wintersburg Channel.

boundary fault zone. The sediments within this portion of the graben were further investigated with nine borings and 72 CPTs (Woodward-Clyde Consultants, 1991).

Cone Penetrometer Tests

CPTs are commonly used for geotechnical site investigations, liquefaction studies, and aquifer characterization (Edelman and Holguin, 1996). A CPT consists of pushing a cylindrical cone-tipped probe into relatively soft, fine-to-coarse–grained sediments or soil while continuously recording the skin friction and penetration resistance of the sediments. CPT signatures used herein were created by plotting the ratio of skin friction to penetration resistance and penetration resistance versus depth (Fig. 3). The grain size of sediments can be identified from their CPT signature (Edelman and Holguin, 1996). Typically, coarse-grained sediments such as sand and gravel have high penetration resistance and a low friction ratio, whereas fine-grained sediments such as silt and clay have low penetration resistance and a high friction ratio. Silty coarse sand would have both moderate penetration resistance and friction ratios. When analyzed together, a group of CPT signatures can be used to identify sedimentary units and map subsurface geology by correlating distinctive units among adjacent CPT holes.

CPTs were conducted along several transects across the fault zone in the study area (Fig. 2) and advanced to 30 m depth. Additional CPTs were conducted outside the fault zone to investigate the lateral continuity and thickness of key marker units. The CPT data were supplemented by nine continuously cored 8-in.-diameter borings to verify lithologic interpretations of the CPT signatures and to collect samples of wood and shell for radiocarbon dating. CPT data were collected at intervals of 3.05 cm, but the vertical resolution of stratigraphy is limited by the discernible vertical variations in grain size of the deposits and thickness of the units. The thinnest units (6, 7, 9, 12, and 14B) have minimum thicknesses of approximately 24 to 42 cm on different cross sections. Therefore, the smallest recognizable vertical offset of the thin-bedded units would be approximately 12 to 21 cm. Recognition of faulting in thicker units, such as unit 14C, would require larger vertical offsets.

The tops of completed CPT holes and borings were surveyed to provide elevation control for constructing cross sections. Uncertainty in the elevation measurements includes precision error of approximately 1 mm and location error of $\leqq$5 cm due to disruption of the ground surface by drilling. Additional information on CPT data collection is presented by Woodward-Clyde Consultants (1991).

Cross Sections

The CPT signatures were plotted in cross-section format to analyze subsurface stratigraphy both within and outside

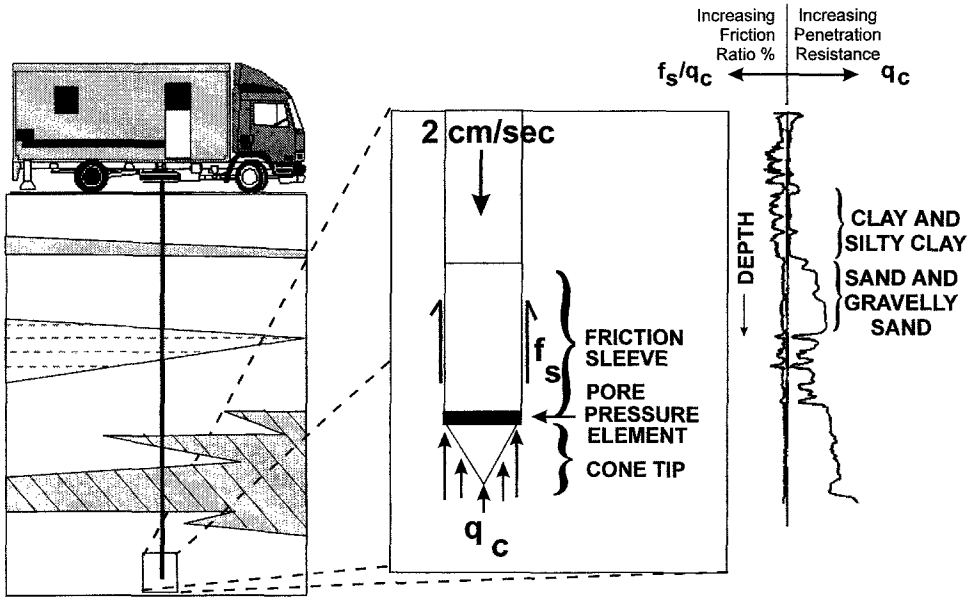

Figure 3. Schematic representation of how CPT data are collected. A 43.7-mm-diameter probe is continuously pushed into sediments with a hydraulic ram mounted inside a 20-ton truck. The probe provides readings of skin friction, f_s, and penetration resistance, q_c, as it is advanced. An electric cable connects the CPT probe to a computer-controlled digital data acquisition system inside the CPT truck. CPT data are plotted versus depth, to obtain a "signature" of the sediment characteristics. The signature is formed by plotting penetration resistance on the right and the ratio of skin friction over penetration resistance on the left. When plotted in cross-section format, CPT signatures can be used to correlate subsurface stratigraphy, similar to interpretation of oil-well E-log data. Modified from Edelman and Holguin (1996).

of the fault zone. Stratigraphic units were mapped by connecting contacts between CPTs. Most sedimentary units can be correlated across each cross section and between the cross sections. Many of the units are also laterally continuous and nearly flat beyond the area of detailed study. Local facies changes cause apparent dips of some contacts. Vertical stacks of upwardly decreasing apparent dips were interpreted as faults (see below). Apparently—dipping units above flat-lying units were interpreted as facies changes. Contacts were projected toward fault zones from adjacent unfaulted areas. Therefore, dips of units within fault zones are not true dips.

Fault Identification

Faults were identified from several types of evidence. The general location of the fault zone in the study site was identified during preliminary studies (Freeman *et al.,* 1992). On the cross sections, faults were recognized by abrupt changes in otherwise laterally continuous units. Faults are interpreted to exist where a vertical sequence of laterally continuous units drop, and change thickness, and/or change lithology. Increasing apparent vertical displacement of units with depth between adjacent CPTs was interpreted as a zone of faulting between the CPTs. Plots of depth versus apparent vertical displacement were prepared for suspected fault zones. The plots confirmed the general trend of increasing displacement with depth and suggested a history of multiple ruptures of several of the fault zones.

The top (upward termination) of a fault was assumed to be overlain by flat-lying units of constant thickness. An interpreted fault between adjacent CPTs may represent a zone of more than one break because resolution of individual faults is limited by the spacing of the CPTs. Spacing of CPTs was limited by land ownership and access constraints.

Some of the features attributed to faulting might be caused by a combination of folding and variations in stratigraphy. However, with a few exceptions (discussed in detail in the Appendix), the interpreted locations of faults cannot be attributed solely to stratigraphic changes. Changes in thickness and lithology of most units are gradual outside the interpreted fault zones. Given the lateral continuity of the units across the site, it would be surprising to have vertically aligned abrupt stratigraphic changes caused solely by depositional processes. Apparent downdropping of units could be explained by either folding or faulting. However, the accompanying changes in thickness of units are more plausibly the result of displacement and deposition over a scarp than folding. In this case, a *scarp* is defined as relief of the ground surface caused by movement on an underlying fault.

Results

Three cross sections spanning the northern part of the graben are shown in Figures 4a, 4b, and 4c. The location of the cross sections is shown in Figure 2. Data from CPTs and borings confirm that the area north of the fault zone is underlain by approximately 20 m of nearly flat, laterally continuous, Holocene-aged strata of sand, silt, clay, and gravel, which were deposited atop late-Pleistocene–aged sand and silt.

The stratigraphy is summarized in Figure 4a. The basal Holocene unit (unit B) is a distinctive, coarse sand and gravel layer with a high penetration resistance. Units 1 through 11 are also well defined and relatively easy to correlate across the study site. Units 12 through 16 are more laterally variable in thickness and lithology.

Nine samples from the borings were radiocarbon dated (Table 1). Radiocarbon dates can be used to estimate the age of the sediments. None of the sample ages are out of temporal sequence, suggesting that contamination by detritus is not a significant problem at the site. The depositional history of the site is revealed by analysis of the stratigraphy and comparison of the elevation of dated samples with sea-level elevation at corresponding times (Fig. 5). Rapidly rising sea level during the early to middle Holocene caused aggradation of fluvial sediments (units B through 8). About 8000 yr ago, the elevation of the site became approximately coincident with sea level. As sea level continued to rise, a brief period of estuarine deposition (units 9 and 10) was followed by deposition in a shallow littoral environment (units 11 through 14). Units 13 and 14 are interpreted to be littoral sands with lateral thickness changes and marine fossils (shells). As sea level stabilized and deposition continued, clay-rich units 15 and 16 were deposited in an estuarine environment. The uppermost 60 cm of sediment were not mapped because they were modified by site development.

Several faults were identified between the CPTs on each cross section. The faults are numbered (e.g., 1A, 1B, 1C on cross section 1; 2D, 2E, etc.) to facilitate discussion. Cross sections 1 and 2 span the northern fault zone boundary of the graben. Cross section 3 includes part of the southern boundary as well as the northern fault zone boundary of the graben. The normal component of motion of the graben faults has caused progressively greater vertical displacement of units with increasing depth. For example, the top of unit B, dated at about 11.7 $\pm$ 0.7 ka (Table 1), has a maximum vertical separation of 3.9 m across the fault zone on cross section 3. Vertical displacement of younger units near the top of the section is minimal.

Interpretation

Paleoseismic Event Recognition

The method used to identify paleoearthquakes on the cross sections is similar to methods used in traditional paleoseismic trench investigations. In trenches, event horizons are identified by changes in elevation, thickness, and lithology of stratigraphic units across a fault. Faulted horizons are covered by less deformed or undeformed units. Although subsurface investigation with CPTs does not allow direct observation of fault zones, the stratigraphic horizons of paleo-

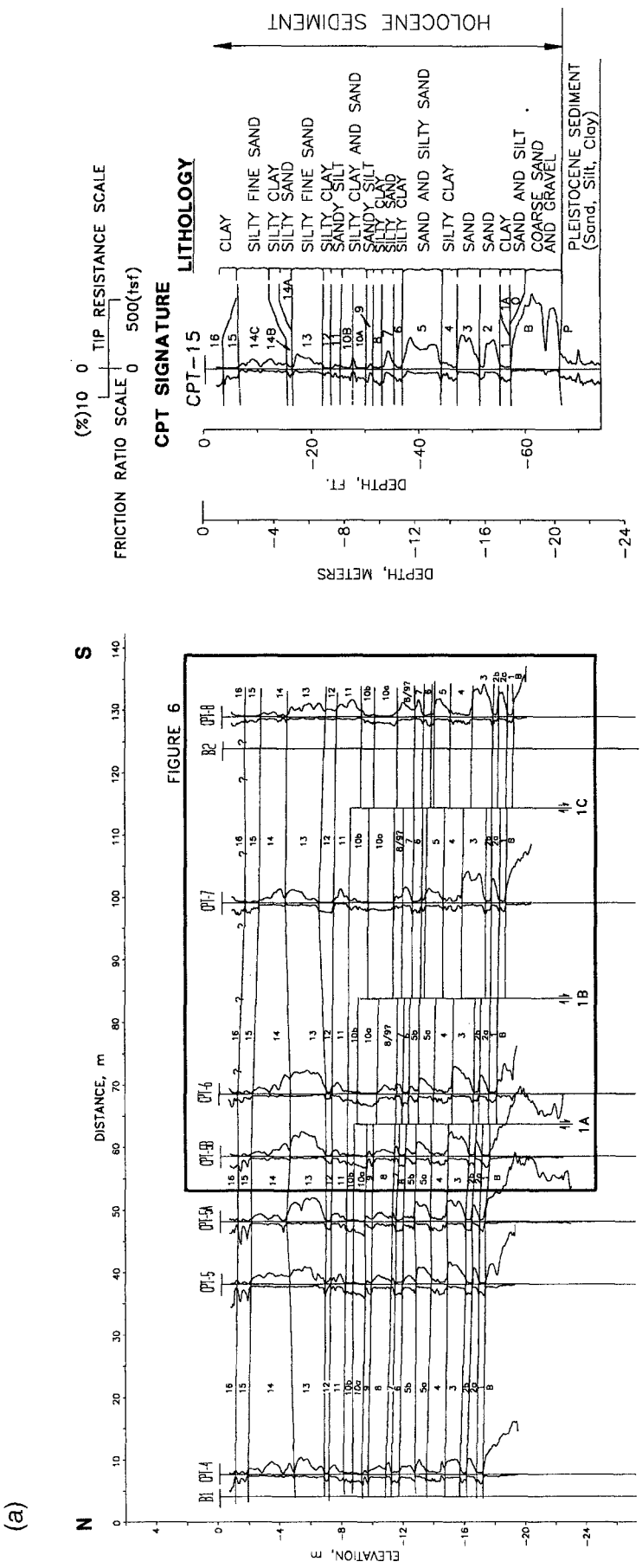

Figure 4. (a) Cross section 1 is plotted with the vertical scale exaggerated. Borings B1 and B2 are coincident with CPTs 4 and 8, respectively, but are shown next to the CPTs for clarity. Refer to Figure 2 for location of cross sections and borings. The location of Figure 6 is enclosed in a box. The lithology and stratigraphy of the site is summarized by a compilation of data from the log of boring B3 and the signature of CPT 15. Lateral thickness changes across the site are shown schematically. The scale of penetration resistance is tons per square foot (tsf).

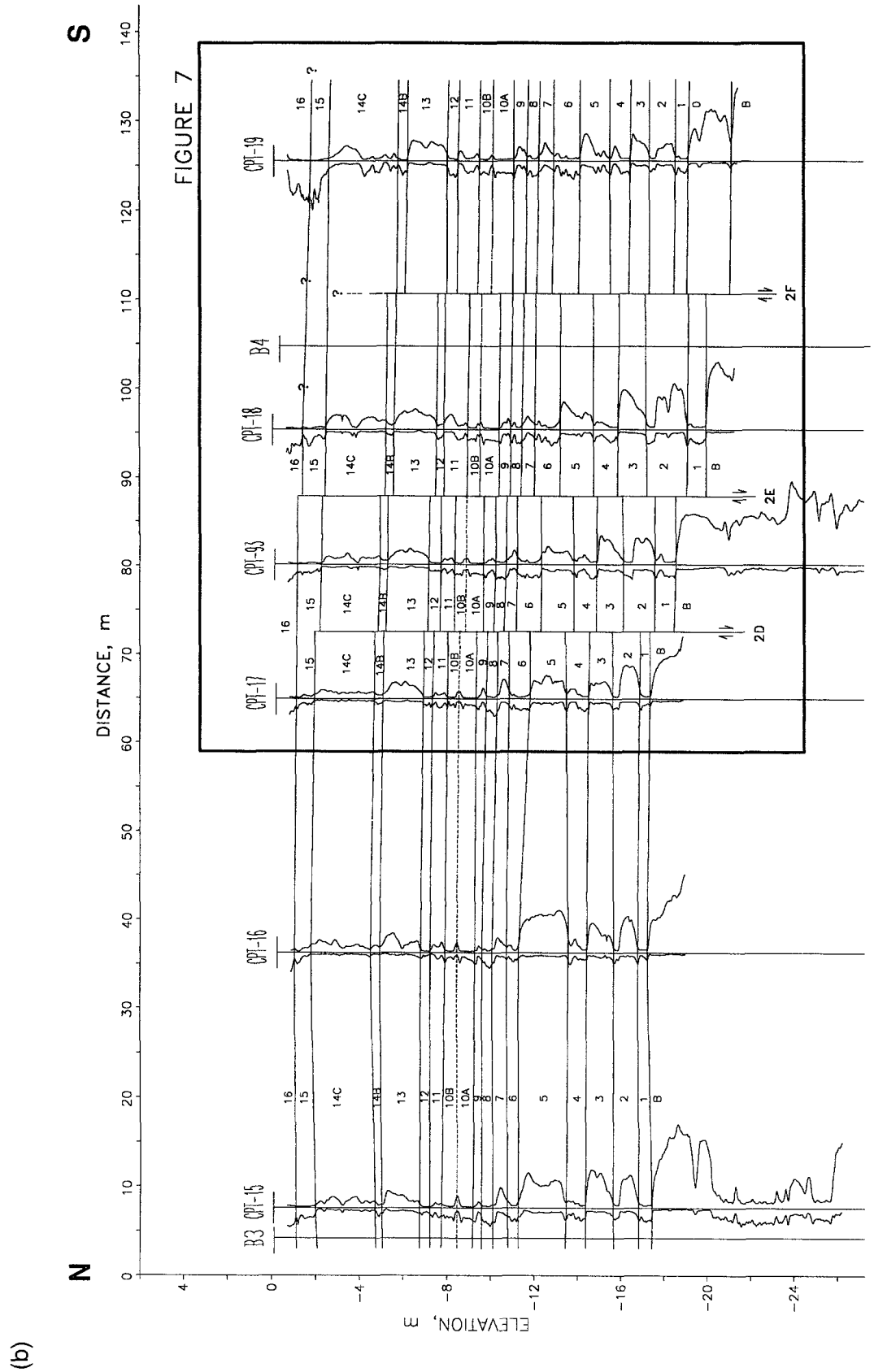

Figure 4. (b) Cross section 2 is plotted with the vertical scale exaggerated. Boring B3 is approximately 18.3 m north of CPT 15, and boring B4 is approximately coincident with CPT 18. Both borings are shown next to the CPTs for clarity. Refer to Figure 2 for location of cross sections and borings. The location of Figure 7 is enclosed in a box.

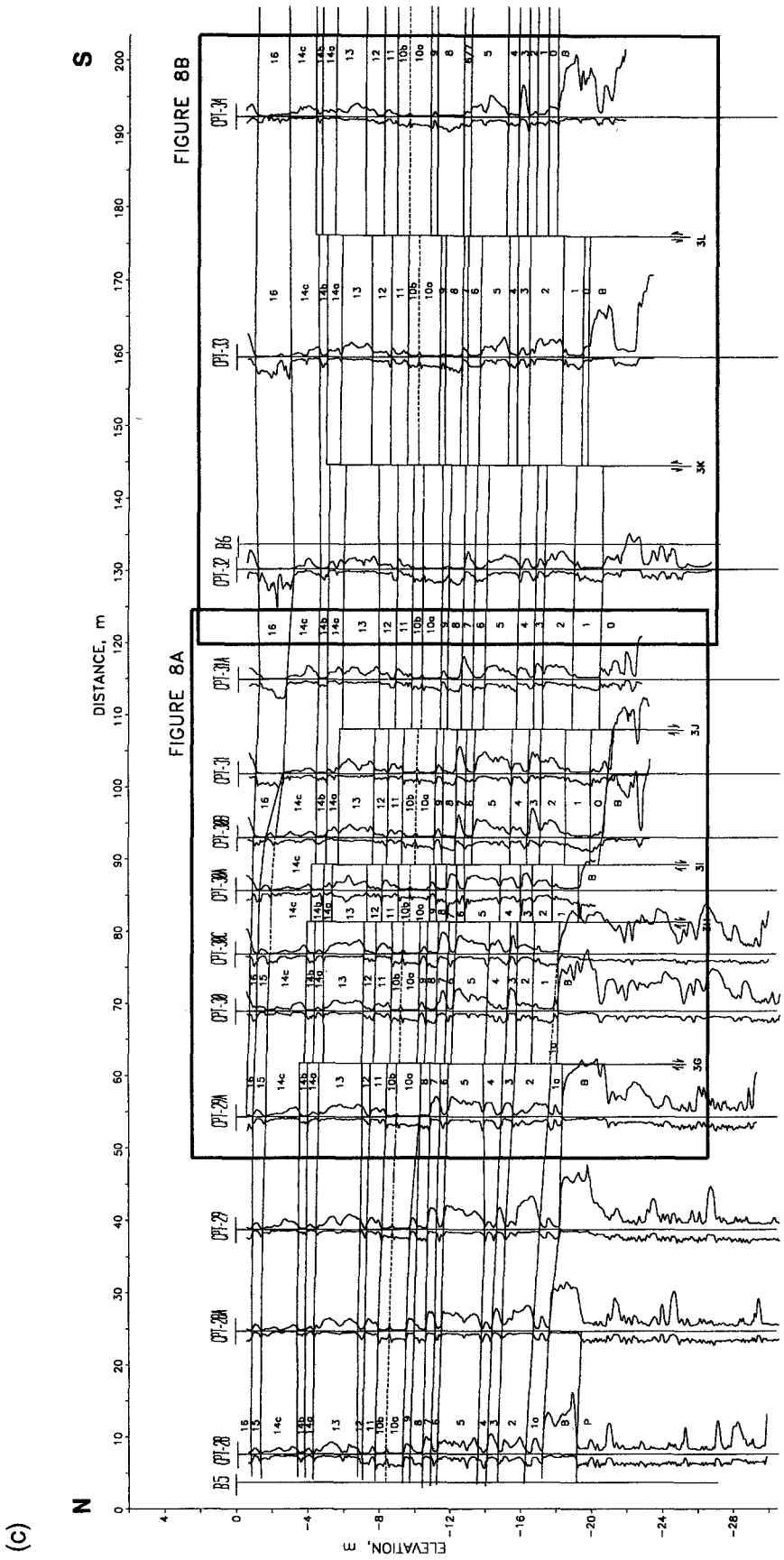

Figure 4. (c) Cross section 3 is plotted with the vertical scale exaggerated. Boring B5 is approximately 7.6 m north of CPT 28 but is plotted next to it. Refer to Figure 2 for location of cross sections and borings. The locations of Figures 8a and 8b are enclosed in boxes.

Table 1
Radiocarbon Dates

Sample	Boring	Elevation (m)	Unit	Radiocarbon Years B.P.* (1σ)	Calibrated Ages ka† (2σ)	Description
Beta-43459	B-9#1	−4.39	14 (?)	4459 ± 130	4.335 + 0.360/−0.405	shell
Beta-43458	B-9#2	−6.84	11 or 12 (?)	5360 ± 80	5.485 + 0.170/−0.195	shell
Beta-42281	B-3#1	−9.39	9/10 contact	7050 ± 80	7.830 + 0.135/−0.170	wood
Beta-42280	B-2#2	−15.70	4	8530 ± 200	9.485 + 0.465/−0.495	wood
Beta-42278	B-1#3	−14.02	4	9330 ± 100	10.335 + 0.455/−0.300	wood
Beta-42285	B-4#3	−15.97	3 or 4	9390 ± 230	10.370 + 0.630/−0.440	wood
Beta-42282	B-3#4	−17.16	1/2 contact	9510 ± 70	10.540 + 0.380/−0.235	wood
Beta-42283	B-3#5	−18.23	B	10100 ± 150	11.680 + 0.650/−0.690	wood
Beta-42286	B-4#4	−23.29	P	>30,770	—	wood

Samples analyzed by Beta-Analytic Inc. of Coral Gables, Florida.
*δ^{13} for Beta-43459 is 0.9 and for Beta-43458, −2.1. δ^{13} for all other samples assumed to be −25. B.P. ages are reported as years before 1950 A.D.
†All ages and errors are rounded to closest 5 yr. Years reported in ka are defined as calendar years before 1950 A.D. Calibrated with CALIB v. 3.0.c (Stuiver and Reimer, 1993). Shell dates are calculated using the marine calibration curve and an R value of 225 ± 35.

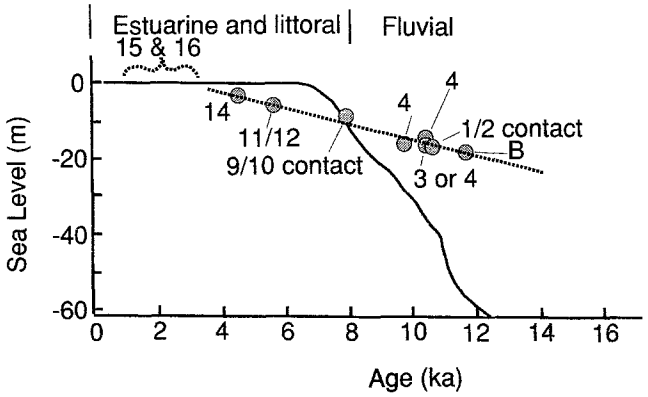

Figure 5. Plot of radiocarbon dates and depths of samples superimposed on global late-Pleistocene/Holocene sea level (compiled from Bard *et al.*, 1990; Chappell and Polach, 1991; Gibb, 1986). The correlated unit and interpreted depositional environment of the samples are labeled.

seismic events can be identified by applying the same criteria.

A recognizable surface rupture is defined for our purposes as a differential vertical displacement of a previous ground surface that is large enough to be recognizable at the resolution of our methods. The minimum thickness of correlatable units (24 to 42 cm) limits the minimum resolvable vertical separation to 12 to 21 cm. Additional uncertainty in elevation measurements (up to 5 cm) increases the minimum resolvable elevation difference to 17 to 26 cm.

Plots of apparent vertical displacement with depth revealed increasing displacement suggestive of multiple-rupture events but were not useful for identifying the stratigraphic horizons of individual events because the faults are right oblique slip rather than pure dip slip. To identify paleoseismic events, it is necessary to evaluate both apparent displacement and changes in stratigraphy. A faulting event can be identified by differential vertical displacement of stratigraphic units and corresponding thickening of a unit due to subsequent deposition, or "ponding," of sediment against a scarp. Lithologic changes across the fault zone may provide additional evidence of an event.

Changes in the amount of apparent vertical displacement across a fault combined with thickening (ponding) of the overlying sedimentary unit on one side of a fault are interpreted as probable evidence of paleoearthquakes. Because there are small lateral changes in thickness of most units, minor changes in lithology are also present on opposite sides of the oblique-slip faults. These changes can either provide additional evidence of an event horizon or make the correlation of units across a fault uncertain. The evidence for each suspected event in each cross section is presented in the Appendix and summarized below.

Cross Section 1

There are three fault zones numbered as 1A, 1B, and 1C in cross section 1 (Fig. 6). There is evidence for at least one paleoearthquake on each fault in cross section 1 and evidence suggestive of two rupture events on fault 1A. The youngest event on fault 1A occurred at the approximate time that the lower part of unit 10 was at the ground surface. The horizon of the event is not well constrained due to stratigraphic changes in units 8 and 9. Similarly, it appears that fault 1B ruptured either unit 8, 9, or the base of unit 10 to form a scarp. Rupture of fault 1C apparently occurred when the top of unit 10 or the lower part of unit 11 was at the ground surface. There is also suggestive evidence that an early Holocene event on fault 1A displaced units 1 and B.

Cross Section 2

Each of the three interpreted faults (2D, 2E, and 2F) on cross section 2 appears to have ruptured at least twice since deposition of unit B. The youngest event on fault 2D apparently ruptured to the top of unit 14c or near the base of unit 15 (Fig. 7). There is good evidence for an older event that broke unit B and suggestive evidence of a third event

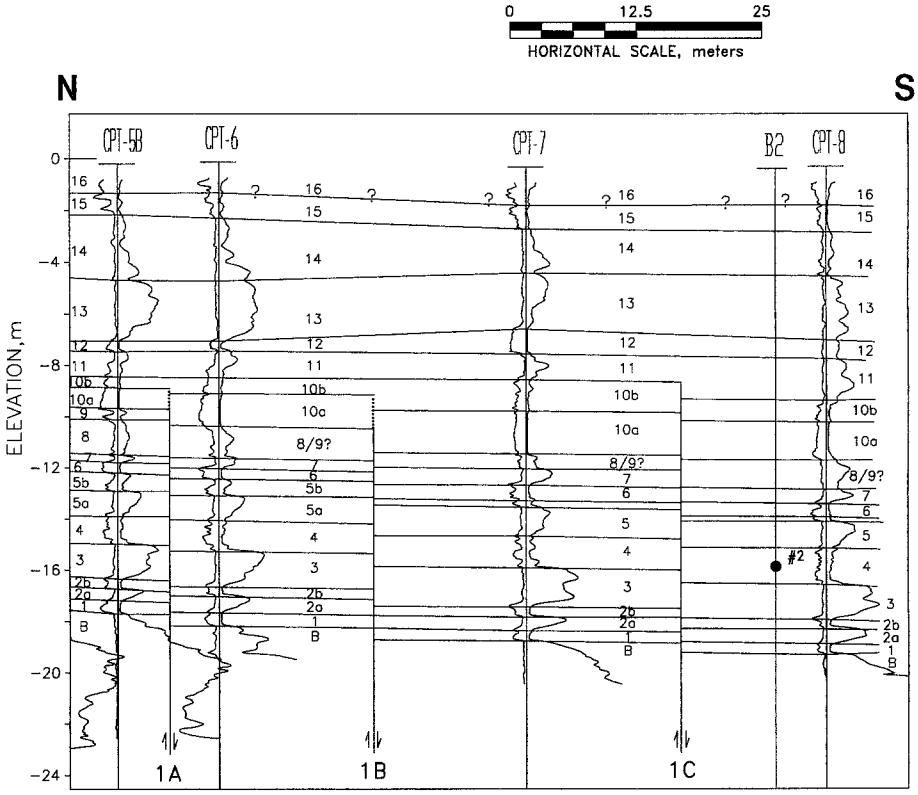

Figure 6. Detail of fault zone in cross section 1. Location of samples for radiocarbon dating is marked by numbered bullets. See Figure 4a for location.

that may have occurred when unit 1 was at the ground surface. Fault 2E may also have moved three times: when unit 1 was at the ground surface, after deposition of unit 10, and possibly very recently. Fault 2E may have ruptured to the top of the section. Fault 2F appears to have moved at least once and possibly twice during the Holocene, most recently when unit 14b was at or near the ground surface. Changes in stratigraphy also suggest that fault 2E ruptured when unit B was at the ground surface, but the evidence is inconclusive.

Cross Section 3

There are six faults interpreted on cross section 3. As shown on Figures 8a and 8b, faults 3G, 3H, 3I, and 3J show down-to-the-south separation, and faults 3K and 3L show the opposite sense of separation. Fault 3G displaces sediment up to unit 14b, suggesting that the most recent event occurred when unit 14b was at or near the ground surface. Fault 3H may have ruptured several times during the Holocene. The youngest event most likely occurred when unit 14b or the lower part of 14c was at the ground surface. Two older events may have occurred when unit 1 was at the ground surface and after deposition of unit 9 or the lower part of unit 10. There is good evidence for at least two events on fault 3I. The youngest event probably occurred when unit 14b or the lower part of unit 14c was at the ground surface. At least one and probably two events, occurred when units B and/or 1 were at the ground surface. Only one event, near the top of unit 13 or the lower part of unit 14, is recognized on fault 3J. Stratigraphic variations and elevation changes suggest that multiple displacements occurred on fault 3K at the approximate horizons of units 0, 3, 6, and 13 or 14. Fault 3L displaces units up to unit 14b. Differential displacement near the base of the section suggests that two older events occurred: after deposition of unit 0 and again after deposition of unit 1.

Number of Paleoearthquakes

Some of the interpreted paleoseismic events discussed above could be artifacts of nontectonic lateral variations in stratigraphy. For example, two apparent events on fault 3K that are not exhibited by other faults are probably caused by stratigraphic variations. However, multiple apparent paleoseismic events at the same stratigraphic horizon on different faults provide stronger evidence that a paleoearthquake occurred at that horizon. To separate paleoearthquakes from stratigraphic variations, the horizons of suspected paleoseismic events on all faults in the three cross sections are plotted for comparison in Figure 9. Surface ruptures most likely occurred at the stratigraphic horizons where there is evidence of paleoearthquakes on multiple faults. Figure 9 shows evidence of at least three surface ruptures in the lower,

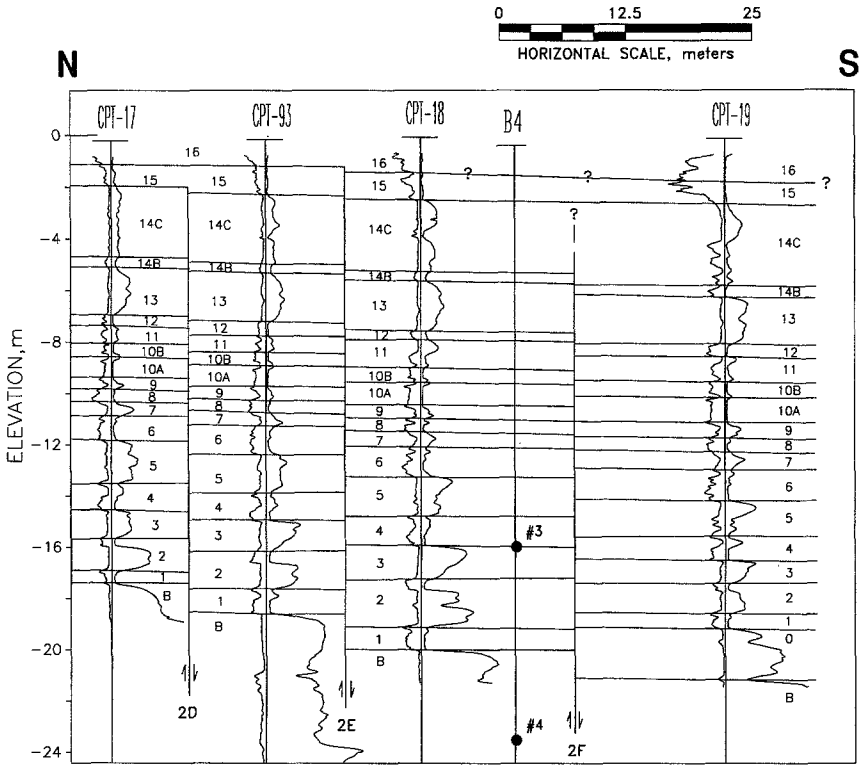

Figure 7. Detail of fault zone in cross section 2. Location of samples for radiocarbon dating is marked by numbered bullets. See Figure 4b for location.

middle, and upper parts of the section. In addition, there is good evidence that two events, rather than just one, ruptured the lower part of the section. The upper part of the section may also have ruptured twice, rather than once, although the number of faulting events near the top of the section is poorly constrained due to lateral stratigraphic variation in the littoral sediments of units 13 and 14. Therefore, a maximum of five and a minimum of three recognizable surface ruptures have occurred within the studied section of the NBF.

Ages of Paleoearthquakes

Radiocarbon dates of samples collected from continuously cored borings were correlated with stratigraphic units to constrain the time of paleoearthquakes. Calibrated radiocarbon dates are plotted on Figure 9 at the sample collection horizons. The oldest recognized paleoseismic events occurred in the early Holocene. The earliest event occurred after deposition of the oldest Holocene sediment (unit B) dated 11.7 ± 0.7 ka and before deposition of the top of unit 1 or the base of unit 2, dated 10.5 + 0.4/−0.2 ka. The second oldest event occurred shortly before, or at approximately the time of deposition of the sample dated 10.5 + 0.4/−0.2 ka. Thus, two early Holocene events may have occurred in the span of approximately 1200 yr.

At least one event occurred in the middle Holocene, at the approximate time that unit 10 was at the ground surface. Two samples (from unit 11 or 12, and from the top of unit 9 or the base of unit 10) constrain the age of this event to between 5.5 ± 0.2 ka and 7.8 + 0.1/−0.2 ka, respectively. The youngest event or events occurred after deposition of the base of unit 14b. A sample tentatively correlated with the base of unit 14 is dated as 4.3 ± 0.4 ka. Therefore, it appears that an event occurred shortly after 4.3 ± 0.4 ka. The presence of a younger near-surface rupture event is suggested. Based on the shallow depth of the apparent rupture termination, such an event could postdate 4.3 ± 0.4 ka by several millenia.

Discussion

1933 Earthquake

The age of the youngest surface rupture along the NBF could not be determined from this study. The epicenter of the 1933 M_w 6.4 Long Beach earthquake was approximately 5 km southeast of the study site (Hauksson and Gross, 1991). The 1933 earthquake most likely occurred on the NBF because the epicenter is approximately coincident with the mapped trace of the Holocene NBF as mapped by Bryant (1988), and because the preferred nodal plane (Hauksson and Gross, 1991) parallels the NBF. The 1933 earthquake caused ground disturbance along the NBF in Orange County, including the study site (Barrows, 1974). However, none of the reported ground deformation was definitively attributed to surface rupture. One reported observation of surface rup-

(a)

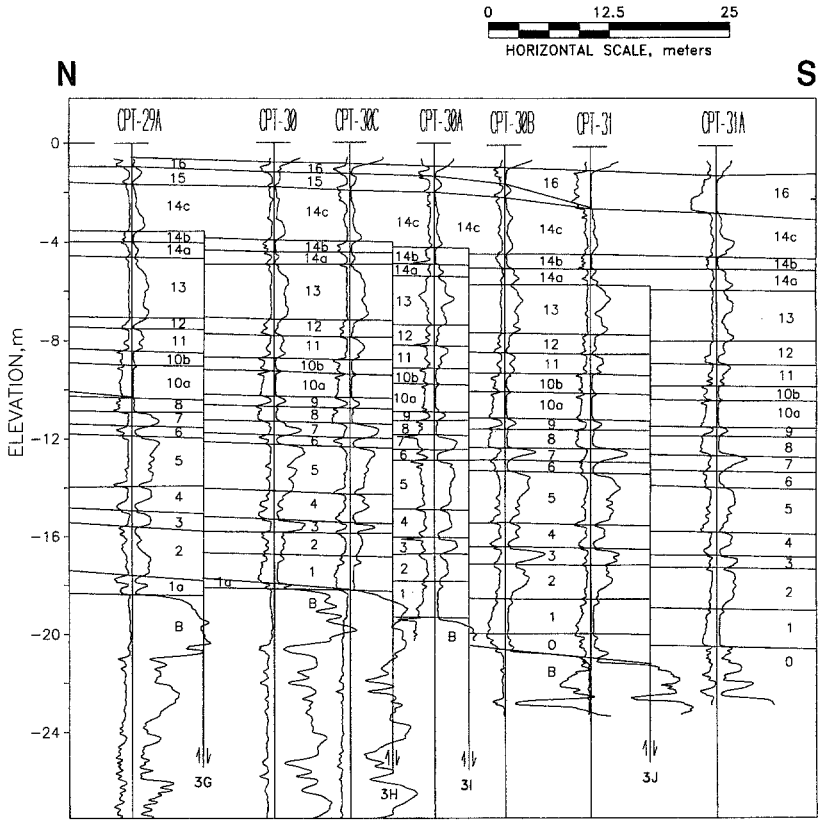

(b)

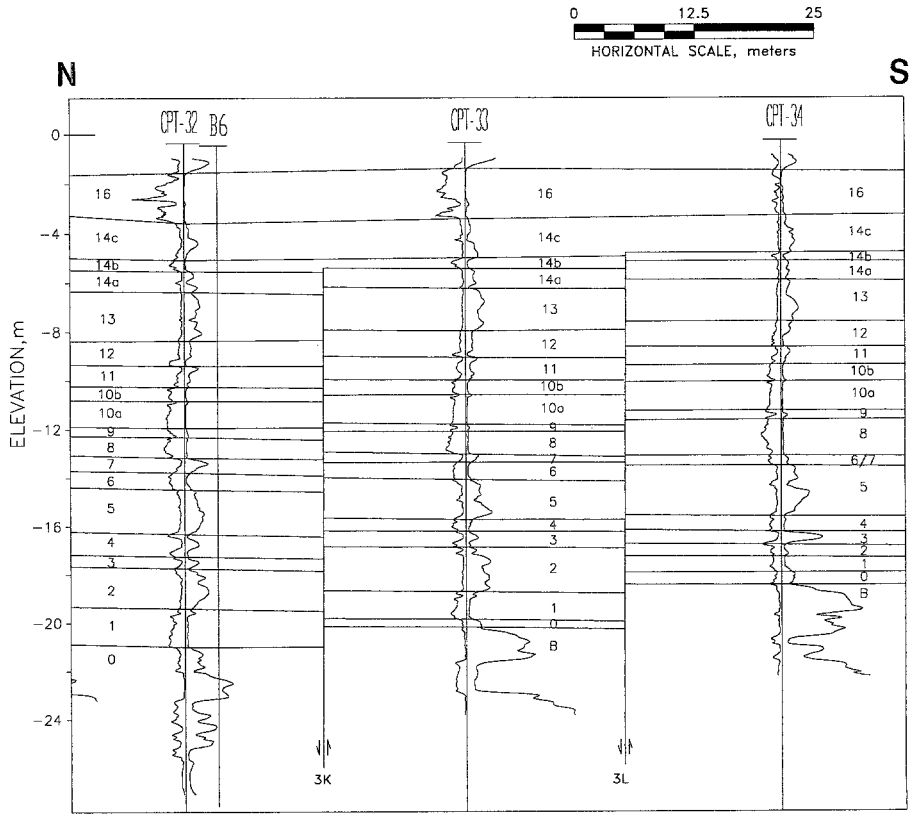

Figure 8. (a) Detail of fault zone in cross section 3. See Figure 4c for location. (b) Detail of fault zone in cross section 3. See Figure 4c for location.

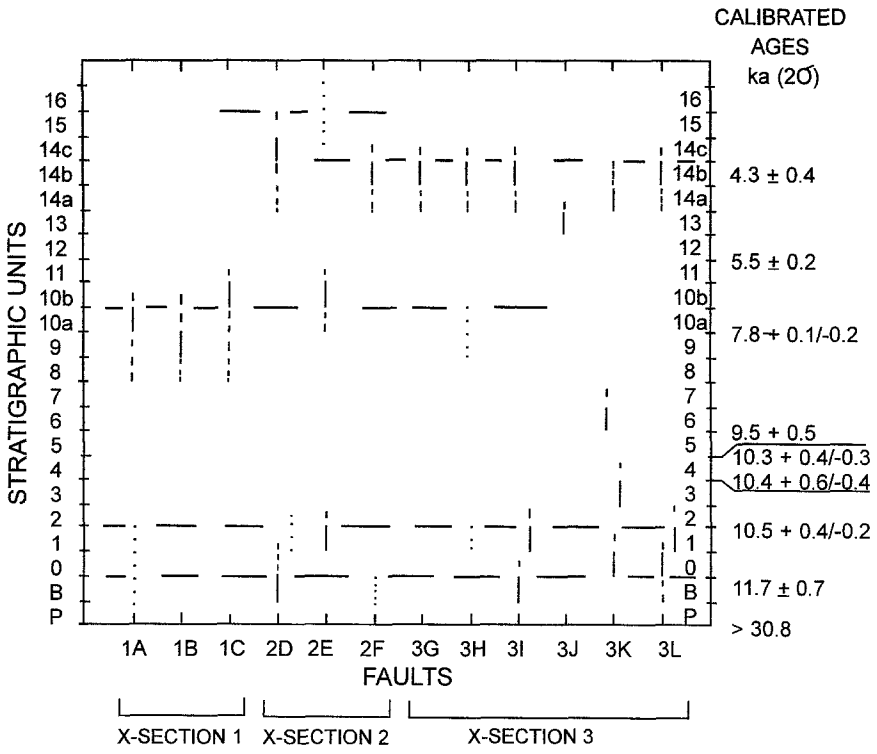

Figure 9. Summary of paleoseismic events. The stratigraphic unit that was apparently at the ground surface at the time of an event is designated with a solid vertical line. Upper and lower limits of confidence are dashed. Suggestive evidence for an event is shown with dots. Dashed horizontal lines show the interpreted stratigraphic level of paleoseismic events. Calibrated radiocarbon dates from several stratigraphic units constrain the ages of the interpreted events.

ture in Newport Beach (Guptill and Heath, 1981) proved inconclusive with further study (Freeman *et al.*, 1992). At the study site, analysis of the CPT cross sections and other data neither preclude nor show convincing evidence of surface rupture within the past millenium.

Size and Number of Paleoearthquakes

Our methods are biased toward recognition of surface ruptures with significant vertical displacement along graben-boundary faults followed by deposition and burial of a scarp prior to significant erosion. Rapidly rising sea level in the early Holocene triggered fluvial aggradation at the site. The aggradation caused sedimentation within the graben and burial of at least some of the scarps. However, a lower sedimentation rate due to slower sea-level rise in the mid to late Holocene was not as favorable for preservation of fault scarps. Therefore, evidence is clearest for three surface ruptures in the early to middle Holocene. Evidence for the two youngest events is not as well expressed, partly because of changes in the stratigraphy of younger sediments. However, a similar, independent, paleoseismic study of the NBF near the Santa Ana River (Shlemon *et al.*, 1995) also concluded that at least five surface ruptures occurred in the Holocene. By analogy, our preferred interpretation is that five significant surface ruptures occurred at our study site during the Holocene.

It is possible that additional smaller surface ruptures and/or strike-slip ruptures with negligible vertical displacement have also occurred during the Holocene and are not recognizable with our methods. For example, if reports are correct that there was no surface rupture at the study site in 1933, then earthquakes similar to the M_w 6.4 1933 earthquake probably would not be identified by our study. The paleoearthquakes identified in this article may have been as large as or larger than the 1933 earthquake because they apparently produced measurable surface rupture localized along a relatively narrow fault zone.

Holocene Slip Rate

The structure of the NIFZ, the long-term right-lateral slip rate, and the displacement of Quaternary sediments (Hazenbush and Allen, 1958; Wilcox, 1971; Barrows, 1974; Freeman *et al.*, 1992; California Dept. of Water Resources, 1968) indicate that the dominant sense of displacement across the NIFZ in the region of the study area is right lateral. The focal mechanism of the 1933 earthquake was dominantly right lateral with a minor normal component (Hauksson and Gross, 1991). At the study site, the presence of a graben in Holocene sediments between right-stepping splays of the

NBF is also consistent with right-lateral Holocene displacement.

If we assume that the paleoearthquakes at the site were at least as large as the 1933 earthquake, then a minimum Holocene slip rate can be estimated based on the source parameters of the 1933 earthquake. The average co-seismic slip of the 1933 earthquake was 85 to 120 cm at depth (Hauksson and Gross, 1991). If this amount of slip is considered to be a minimum amount of surface slip in each of the five suspected Holocene paleoseismic events, then the minimum Holocene slip rate would be approximately 0.35 to 0.55 mm/yr. If three comparable-sized paleoearthquakes occurred, the minimum Holocene slip rate would be 0.21 to 0.33 mm/yr. However, as explained above, we prefer five Holocene events to three, so our preferred minimum rate is 0.35 to 0.55 mm/yr.

This minimum rate is approximately 10 times greater than the slip rate estimated at Signal Hill (Fig. 1; Suppe *et al.,* 1992) but is substantially less than the 1.1 to 2.0 mm/yr Holocene slip rate of the Rose Canyon fault (Lindvall and Rockwell, 1995). Shlemon *et al.* (1995) estimate a total Holocene slip rate of 1.5 to 2.5 mm/yr for the NBF near the Santa Ana River, based on the vertical displacement of early-Holocene sediments and an estimate of the ratio of horizontal to vertical displacement (6 to 10). At our study site, the apparent vertical displacement (2.0 to 3.9 m) of the basal Holocene unit (11.7 ± 0.7 ka) yields an *apparent* vertical slip rate of 0.16 to 0.35 mm/yr. Applying the same estimated components of motion would yield a right-lateral Holocene slip rate of 1.0 to 3.5 mm/yr, consistent with the rate of Shlemon *et al.* (1995) near the Santa Ana River. Because this slip rate is derived from a vertical separation rate within a graben, and estimated components of motion, it should not be misconstrued as a true slip rate. However, it is interesting because it suggests that the total slip rate is several times larger than the minimum 0.34 to 0.55 mm/yr Holocene rate and could be as high as the slip rate of the Rose Canyon fault.

Recurrence

The dates of paleoearthquakes on the NBF suggest that the recognized surface ruptures were not regularly spaced in time, but the dates of events are too poorly constrained to rigorously test this hypothesis. The two oldest Holocene events apparently occurred within approximately 1200 yr of each other, and at least three millennia passed between the early- and middle-Holocene events. Therefore, Holocene paleoearthquakes on the NBF may have occurred in temporal clusters, as has been reported for other faults (Grant and Sieh, 1994; Marco *et al.,* 1996; Hiryabayashi *et al.,* 1996).

Conclusions

Application of cone penetrometer testing is a promising method for studying subsurface fault zones in stratified, unconsolidated sediment where urbanization, access restrictions, or high water tables make trenching unfeasible. Our results show that the North Branch of the Newport–Inglewood fault zone has generated at least three and most likely five recognizable surface ruptures in the past 11.7 ± 0.7 ka in Huntington Beach, California. Additional smaller earthquakes similar to the M_w 6.4 1933 Long Beach earthquake may also have occurred but are not recognizable with this method. The minimum right-lateral Holocene slip rate of the NIFZ in coastal Orange County is estimated to be 0.34 to 0.55 mm/yr. The actual slip rate may be significantly higher.

Acknowledgments

Many people contributed to preliminary work that led to this study. We especially thank C. Sykes, G. Johnpeer, T. Freeman, and E. Heath for their contributions. Reviews by K. Kelson, R. Wheeler, and an anonymous reviewer substantially improved the manuscript. This work was supported by the Southern California Earthquake Center (SCEC), a Science and Technology Transfer Center funded by the National Science Foundation, U.S. Geological Survey, and Federal Emergency Management Agency. This is SCEC Contribution Number 290.

References

Bard, E., B. Hamelin, and R. G. Fairbanks (1990). U-Th ages obtained by mass spectrometry in corals from Barbados: sea level during the past 130,000 years, *Nature* **346,** 456–458.

Barrows, A. G. (1974). A Review of the Geology and Earthquake History of the Newport–Inglewood Structural Zone, Southern California, *Calif. Div. Mines Geol. Spec. Rept. 114.*

Bryant, W. A. (1988). Recently Active Traces of the Newport-Inglewood Fault Zone, Los Angeles and Orange Counties, California, *Calif. Div. Mines Geol. Open-File Rept. 88–14.*

California Department of Water Resources (1968). Sea water intrusion: Bolsa-Sunset area, Orange County, *Calif. Dept. Water Res. Bull. 63–2.*

California Division of Mines and Geology (1988). Planning Scenario for a Major Earthquake on the Newport-Inglewood Fault Zone, *Special Publication 99.*

Chappell, J. and H. Polach (1991). Post-glacial sea-level rise from a coral record at Huon Peninsula, Papua New Guinea, *Nature* **349,** 147–149.

Edelman, S. H. and A. R. Holguin (1996). Cone Penetrometer Testing for characterization and sampling of soil and groundwater, in *Sampling Environmental Media ASTM STP 1282,* J. H. Morgan (Editor), American Society for Testing Materials, Philadelphia, Pennsylvania (in press).

Freeman, S. T., E. G. Heath, P. D. Guptil, and J. T. Waggoner (1992). Seismic Hazard Assessment, Newport-Inglewood Fault Zone, in *Engineering Geology Practice in Southern California,* B. W. Pipkin and R. J. Proctor (Editors), Assoc. of Engineering Geologists, Star Publishing Company, Belmont, California, 211–231.

Gibb, J. G. (1986). A New Zealand regional Holocene eustatic sea-level curve and its application to determination of vertical tectonic movements, *Bull. Roy. Soc. New Zealand* **24,** 377–395.

Grant, L. B. and K. Sieh (1994). Paleoseismic evidence of clustered earthquakes on the San Andreas fault in the Carrizo Plain, California, *J. Geophys. Res.* **99,** B4, 6819–6841.

Guptill, P. D. and E. G. Heath (1981). Surface faulting along the Newport-Inglewood zone of deformation, *Calif. Geol.* **34,** 142–148.

Hauksson, E. (1987). Seismotectonics of the Newport-Inglewood fault zone in the Los Angeles basin, southern California, *Bull. Seism. Soc. Am.* **77,** 539–561.

Hauksson, E. and S. Gross (1991). Source parameters of the 1933 Long Beach earthquake, *Bull. Seism. Soc. Am.* **81,** 81–98.

Hazenbush, G. C. and D. R. Allen (1958). Huntington Beach Oil Field, *Calif. Div. Oil Gas, Summary of Operations, California Oil Fields,* **44,** 13–23.

Hill, M. L. (1971). Newport-Inglewood Zone and Mesozoic Subduction, California, *Geol. Soc. Am. Bull.* **82,** 2957–2962.

Hirabayashi, C. K., T. K. Rockwell, S. G. Wesnousky, M. Stirling, and F. Suarez-Vidal (1996). A neotectonic study of the San Miguel Vallecitos fault, Baja California, Mexico, *Bull. Seism. Soc. Am.* **86,** 1770–1783.

Lindvall, S. C. and T. K. Rockwell (1995). Holocene activity of the Rose Canyon fault zone in San Diego, California, *J. Geophys. Res.* **100,** B12, 24121–24132.

Marco, S., M. Stein, A. Agnon, and H. Ron (1996). Long term clustering: a 50,000 year paleoseismic record in the Dead Sea graben, *J. Geophys. Res.* **86,** 6179–6191.

Petersen, M. D. and S. G. Wesnousky (1994). Fault slip rates and earthquake histories for active faults in southern California, *Bull. Seism. Soc. Am.* **84,** 1608–1649.

Poland, J. F., A. M. Piper, *et al.* (1956). Ground water geology of the coastal zone Long Beach–Santa Ana area, *U.S. Geol. Surv. Water Supply Paper 1109,* 162 pp.

Shlemon, R. J., P. Elliott, and S. Franzen (1995). Holocene displacement history of the Newport-Inglewood, North Branch fault splays, Santa Ana Rivever floodplain, Huntington Beach, California (abstract with programs), Fall Meeting, *Geol. Soc. Am.* 103.

Stuiver, M. and P. J. Reimer (1993). Extended 14C database and revised CALIB 3.0 14C age calibration program, *Radiocarbon* **35,** 215–230.

Suppe, J., R. E. Bischke, and J. Shaw (1992). Regional map view and cross-sectional determination of fault geometry and slip for blind thrusts in populated areas of southern California, Southern California Earthquake Center 1992 Report, SCEC Annual Meeting 8–9 October 1992, C35–C40.

Wilcox, R. E., T. P. Harding, and D. R. Seely (1973). Basic wrench tectonics, *Am. Assoc. Petroleum Geol. Bull.* **57,** 74–96.

Woodward–Clyde Consultants (1987). Evaluation of Hazards Due to Surface Fault Rupture at Bolsa Chica Mesa and in the Bolsa Chica Lowland, Orange County, California, unpublished technical report prepared for Signal Landmark, Inc., and Orange County Environmental Management Agency.

Woodward–Clyde Consultants (1991). Addendum No. 1 to Woodward–Clyde Consultants October 1987 Report: Evaluation of Hazards Due to Fault Surface Rupture at Bolsa Chica Mesa and in the Bolsa Chica Lowland Orange County, California, unpublished technical report.

Wright, T. L. (1991). Structural geology and tectonic evolution of the Los Angeles basin, in *Active Margin Basins,* K. T. Biddle (Editor), *Am. Assoc. Petrol. Geol. Mem.* **52,** 35–134.

Appendix—Detailed Descriptions of Paleoseismic Events

Cross Section 1

Cross section 1 (Fig. 4a) is an excerpt of a longer cross section that spans the northern margin of the graben boundary. The northern half of cross section 1 shows a nearly flat, unfaulted section of layered sediments. Sediments in the southern half of the cross section have been displaced downward by faulting along the northern margin of the graben step-over. Detail of the fault zone is shown in Figure 6. Based on apparent vertical displacement and changes in stratigraphy, there are three fault zones between CPTs 5B and 6, 6 and 7, and 7 and 8.

Fault 1A is the northernmost fault in the graben. At least one and possibly two events may have occurred on fault 1A. There is progressive downward displacement on fault 1A from the base of unit 10 to unit B. Units 11 and 12 appear to be continuous across unit 10, suggesting that they are unfaulted. Similarly, units 13 and 14 do not appear to be faulted, although their coarse texture would make fault recognition difficult. The apparent termination of the fault zone below unit 11 suggests that a faulting event occurred prior to deposition of unit 11. The stratigraphy on either side of fault 1A is very similar except in units 8 thru 10. Unit 10 is substantially thicker on the south side of fault 1A. The lower part of unit 10, unit 10a, is thicker than the upper part of unit 10 (10b), suggesting that the middle of unit 10 was deposited (ponded) against a fault scarp and then covered with unit 10b. However, a scarp could have formed by surface faulting of unit 8 or 9 and then been buried by unit 10. The event horizon is not well constrained because of stratigraphic changes in units 8 and 9. To the north of fault 1A, units 8 and 9 are mapped as separate stratigraphic units. South of fault 1A, they are not distinguishable as separate units, and the contact with the base of unit 10 is not well defined.

The apparent vertical displacement of units B and 1 suggests that they were faulted by an earlier event. The top of units 1 and B are vertically displaced approximately twice as much as units 2 thru 10. However, since unit 2 is not significantly thicker on the downthrown side of the fault, the evidence for this event is considered suggestive.

Fault 1B displaces units B thru 10a down to the south. The apparent vertical displacement does not increase with depth, suggesting that fault 1B was formed by a single event. Unit 11 appears to be unfaulted, and changes in units 12 through 14 are attributed to facies changes rather than faulting. As with fault 1A, there are changes in facies and thickness of units 8, 9, and 10 across the fault zone. The lower part of unit 10 is significantly thicker on the south side of fault 1B, suggesting that unit 10a was ponded against a scarp formed by faulting of unit 8/9. The scarp could have formed when units 8, 9, or the base of 10 were at the ground surface.

Fault 1C also displaces units B thru 10. The contact between units 11 and 12 appears to be unfaulted because it is horizontal across cross section 1. Therefore, the apparent dip between units 12 and 13 is attributed to a facies change. Thickening of unit 11 south of fault 1C suggests that unit 11 could have been deposited against a scarp created by faulting of unit 10. Unit 8/9 is also thicker on the south side of the fault. However, unit 10 is slightly thinner, and the combined thickness of units 8/9 and 10 is approximately constant across fault 1C. This suggests that faulting occurred when the top of unit 10 or the lower part of unit 11 was at the ground surface.

Cross-Section 2

Cross section 2 (Fig. 4b) spans the northern margin of the graben. The northern half of cross section 2 shows an unfaulted section of layered sediments. Sediments in the southern half of the cross section have been downfaulted

along the northern margin of the graben step-over. Three fault zones on cross section 2 are discussed below and are shown in more detail in Figure 7.

Fault 2D is the northernmost graben boundary fault in cross section 2. The stratigraphic units on either side of fault 2D are very similar, allowing a high degree of confidence in the correlations. The amount of apparent vertical displacement of units increases progressively with depth, indicating multiple-faulting events. Analysis of the stratigraphy and apparent vertical displacements suggests that at least two and possibly three faulting events have occurred on fault 2D. First, the top of unit B is displaced almost twice as much as the top of unit 1, suggesting that an event occurred when unit B was at the ground surface. The overlying unit 1 is nearly twice as thick on the south side of the fault, suggesting that it was deposited against a scarp. A second event may have occurred when unit 1 was at the ground surface, but the evidence for the younger event is not as compelling. The top of unit 1 is displaced more than the tops of units 3 through 14 but less than the top of unit B. Additionally, the overlying unit 2 is slightly thicker on the south side of the fault zone, suggesting that it was deposited over a scarp. The youngest event appears to have ruptured close to the top of the section. The base and top of unit 14c, and all units below 14c, are at a lower elevation on the south side of fault 2D, suggesting that the youngest event ruptured to the top of unit 14c or near the base of unit 15. The top of unit 15 does not appear to be displaced.

Differential displacement and thickening of units across *fault 2E* also indicate displacement by at least two, and possibly three, faulting events. The amount of apparent vertical displacement increases with depth across fault 2E. Units B and 1 are displaced more than younger units. Constant thickness of unit 1 and equal displacement of units B and 1 across the fault suggest that both units were downfaulted by the same event when unit 1 was at the ground surface. Thickening of unit 2 across the fault suggests that it was deposited over a scarp. A younger event is strongly suggested by a significant decrease in the amount of vertical displacement above unit 11 and a significant thickening of unit 11 across the fault. This suggests that unit 10, or the base of unit 11, was faulted, formed a scarp at the ground surface, and was subsequently buried. Minor apparent vertical displacement of all mappable units above unit 11 suggest that faulting in the most recent event may have extended to the top of the section; however, facies changes in units 15 and 16 make the location of the contact and highest level of faulting uncertain.

Fault 2F appears to have moved at least once, and possibly twice, during the Holocene. Units B through 14b appear to be downdropped to the south, suggesting that the most recent event occurred when unit 14b was at or near the ground surface. Unit 14c is thicker on the south side of fault 2F, suggesting that it was deposited over a scarp. The top of unit 14c is similar on both sides of the fault zone, but there are facies changes in the lower part of unit 14c. This further suggests that lower unit 14c was deposited on a scarp. The contact between units 14c and 15 does not appear to be faulted.

Changes in the stratigraphy in the lower part of the section suggest that the top of unit B may be an event horizon. However, changes in stratigraphy and the appearance of unit 0 across fault 2F create uncertainty in correlations and event identification. The top of unit B is displaced downward across the fault more than any of the younger units, suggesting that the top of unit B is an event horizon. A layer of sand between units B and 1, unit 0, was deposited on the south side of the fault. The stratigraphic position of unit 0 suggests that it was deposited on the downthrown side of fault 2F. The CPT signatures of unit 1 are very similar on both sides of the fault, allowing high confidence in correlation of this unit. However, unit 1 is *higher* on the south side of the fault than on the north side, suggesting a sense of motion opposite the direction of displacement of other units. This apparent contradiction could be caused by a large strike-slip component of motion in later faulting event(s), or significant facies changes in the lower stratigraphic units. Either explanation decreases confidence in the interpretation of an event at the top of unit B.

Cross Section 3

Cross section 3 spans the northern and central portions of a graben, as shown in Figure 4c. Apparent vertical displacement across faults 3G, 3H, 3I, and 3J (shown in detail in Fig. 8a) is down to the south. Apparent displacement across faults 3K and 3L (shown in detail in Fig. 8b) is down to the north. Most of the faults in cross section 3 show evidence of movement during the early Holocene and/or when unit 14 was near the ground surface.

Fault 3G appears to displace sediments up to unit 14b. Unit 15 appears to be flat and of constant thickness on both sides of the fault. Therefore, the top of unit 14b or the lower part of unit 14c was most likely the ground surface during the most recent faulting event. There are significant changes in lithology, thickness, and elevation of units B, 1, and 2 on either side of fault 3G. The coarse texture of these units and the apparent pinchout of unit 1a suggest that the differences were caused by fluvial channels rather than faulting.

The stratigraphy on both sides of *fault 3H* is very similar. An increase in displacement with depth indicates that fault 3H moved more than once. Units B through 14b appear to be faulted, based on apparent vertical displacement. Units 15 and 16 do not appear to be faulted, although lateral changes in both units could obscure evidence of an event. Therefore, the youngest faulting event most likely occurred when unit 14b or the lower part of unit 14c was at the ground surface. Small changes in displacement with depth and minor changes in stratigraphy permit the interpretation of two older events, but the evidence is only suggestive. An increase in the amount of apparent vertical displacement below unit 10 and a minor increase in the thickness of unit 10 on the south side of fault 3H suggest that an older event may

have occurred when unit 9 or the base of unit 10 was at the ground surface. Similarly, an increase in apparent displacement and thickening of unit 2 suggests that the oldest event occurred when unit 1 was at the surface.

There is good evidence for the occurrence of at least two events on *fault 3I.* As with faults 3G and 3H, the most recent event probably occurred when unit 14b or the lower part of unit 14c was at the ground surface. This interpretation is based on the apparent vertical displacement of units B through 14b. The apparent displacement of units 3 through 14b is approximately the same. Unit 1 is displaced nearly twice as much as the units above, and the top of unit B is downdropped nearly twice as much as the top of unit 1. This suggests that at least one and probably two events occurred when units B and/or 1 were at the ground surface. Unit 0 was probably deposited against a scarp from the earlier event. The greater thickness of unit 2 on the south side of the fault suggests that it was also deposited over a scarp formed by the faulting of unit 1.

Differences in elevation of units on either side of *fault 3J* suggest that at least one faulting event has occurred. Changes in the amount of apparent vertical displacement and thickness of units across fault 3J are not large enough to discriminate multiple events. All units below the top of unit 13 are at lower elevation on the south side of fault 3J. Unit 14b is approximately the same thickness and elevation on both sides of the fault, suggesting that the most recent event ruptured upward through unit 13, and possibly into the lower part of unit 14a, but did not reach units 14b or 14c.

Fault 3K is near the center of the graben. It displaces sediments downward to the north. Differences in elevation of stratigraphic units suggest that fault 3K has displaced sediments up to unit 14a. Units 14c and 16 are of constant thickness and nearly flat, suggesting that they are not faulted. Therefore, the youngest event on fault 3K probably occurred when either unit 14a or unit 14b was at the ground surface. Multiple movements of fault 3K are suggested by the apparent increase in vertical displacement with depth, and the greater thickness of units 1, 4, and 7 on the north side of the fault. The oldest Holocene event may have occurred before unit 1 was deposited. The base of unit 1 is downdropped across the fault approximately 50% more than the base of unit 2, and unit 1 is substantially thicker to the north, suggesting that it was deposited over a scarp. Thus, an event may have occurred when unit 0 or the base of unit 1 was at the ground surface. By the same logic, two more events could have occurred after units 3 and 6 were deposited. Unit 3 is displaced more than the units above it, and unit 4 is thicker to the north, suggesting that it was deposited over a scarp. Similarly, unit 6 is displaced more than younger units, and the thickness of unit 7 could be explained by deposition over a scarp.

Fault 3L displaces units up to unit 14b, suggesting that the youngest event occurred after deposition of unit 14b or the base of unit 14c. Stratigraphic changes indicate that earlier events displaced the units near the base of the section. The top of unit 0 is displaced 3 to 10 times more than units 3 through 14, suggesting that an event occurred after deposition of unit 0. Overlying unit 1 is nearly twice as thick on the north side of the fault, providing further evidence of a faulting event after deposition of unit 0 or the base of unit 1. Similarly, there is evidence for an additional event after deposition of unit 1, though this evidence is less compelling. The top of unit 1 is displaced less than the top of unit 0 but more than the top of units 2 through 14. In addition, unit 2 is three times thicker on the north side of the fault than on the south side, suggesting that it was deposited over a scarp. Above unit 2, the amount of apparent vertical displacement of units does not show a consistent pattern, suggesting that the youngest event may have had a substantial component of strike-slip motion.

Division of Natural Sciences
Chapman University
Orange, California 92668
Tel.: (714) 744-7697; fax: (714) 532-6048; E-mail: lgrant@chapman.edu
(L.B.G.)

Woodward-Clyde Consultants
2020 E. First Street, Suite 400
Santa Ana, California 92705
(L.B.G., J.T.W.)

Department of Geological Sciences
San Diego State University
San Diego, California 92182
(T.K.R., C.V.S.)

Central Washington University
Ellensburg, Washington 98926
(C.V.S.)

Manuscript received 20 February 1996.